

D. Lee, W.-A. Chen, T.-W. Huang, S.-J. Liu\*

Department of Mechanical Engineering, Chang Gung University, Tao-Yuan, Taiwan, ROC

# Factors Influencing the Warpage in In-Mold Decoration Injection Molded Composites

This report studied, both experimentally and numerically, the factors affecting the warpage in in-mold decoration (IMD) injection molded parts. All experiments were conducted on an 80-ton injection-molding machine. The materials used in the experiments included poly(ethylene terephthalate) (PET) films and 30 % glass fiber-filled PET resins. U-shaped plate parts with three different angles ( $90^\circ$ ,  $135^\circ$ , and  $150^\circ$ ) at the corners were molded. The influence of various processing parameters on part warpage was investigated using an experimental matrix, with its design based on the experimental-parameter-design method developed by Taguchi. The experimental results suggested that all molded parts warped toward the side of the decoration film. For the parameters selected in the experiments, the corner angle and the melt injection pressure were found to be the principal factors affecting the warpage of IMD injection molded parts. The  $90^\circ$  angled parts exhibited the greatest amount of warpage, while the  $150^\circ$  angled parts showed the least amount of warpage. Additionally, a commercially available code (Moldex<sup>®</sup> 3-D) was used to simulate the temperature distribution during the filling process and the molded part warpage. Calculated warpage satisfactorily matched with the experimental data. It has been shown that the warpage of IMD injection molded parts is mainly caused by the imbalanced temperature distribution during cooling, due to the part geometry and the decoration films.

## 1 Introduction

In-Mold Decoration (IMD) injection molding is the process of over-molding on decorated thermoplastic film or applying an overlay of melted thermoplastic material (Defosse, 2001). During the molding process, a film bearing the desired decoration pattern is first formed by a thermoforming process. After trimming, the film is placed in an open mold and held in the desired position (Fig. 1A). The mold then closes, and molten polymer is injected into the cavity where it conforms to the shape of an object (Fig. 1B). Once the object is ejected from the mold, the graphics on the film cannot be removed, as the cooled object and film form a single unit (Fig. 1C) (Wong et al., 1997; Leong

et al., 2007; Liu et al., 2012; Puentes et al., 2009). IMD can achieve different colors, effects, and textures when the part comes out of the mold. It also provides other advantages, including: 1) producing durable, long-lasting graphics, 2) adding back lighting behind a text or logo in one operation, 3) creating different designs without costly re-tooling, 4) eliminating the tactility of conventional labels on parts' surfaces and secondary painting, and 5) molding recycled materials under the decorative film for more cost-effective production. Typical applications of IMD include: automotive interior parts, cellular phone cases, logo imprinted plastic products, etc.

Despite the advantages provided by IMD injection molding, there are some unresolved problems associated with this process that confounds the overall success of this technology. Part warpage is one of them. The warpage of a plastic product can be seen as primarily due to non-uniform differential shrinkages within the product, which leads to the development of uneven residual stresses within the product. As cooling causes the temperature of the injection molded part to decrease, residual stresses are formed inside the part. Prior to the opening of the mold, no out-of-plane warpage is allowed; however, in-plane shrinkage does occur, which relaxes somewhat because of the constraints. Once the whole part is completely solidified after ejection, the part is allowed to warp out-of-plane, and warpage is observed because of the temperature imbalance during the cooling process. The imbalanced cooling is enhanced due to the presence of the decoration film in IMD injection molding. In order to predict the residual stress and warpage in a polymer product, one must account for the effect of the processing conditions, the material behavior, and the geometric effects. Presently, various research has examined the following: the warpage of conventionally injection molded parts, including warpage in glass beads filled composite parts (Kovacs and Solyomossy, 2009), stiffened plates (Lee et al., 2010), and thin wall parts (Ozcelik and Sonat, 2009; Chiang et al., 2011); modeling and simulation (Liu et al., 2009; Zhou et al., 2011a,

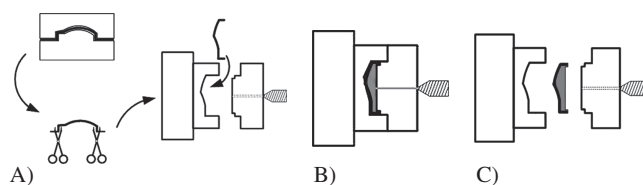


Fig. 1. The in-mold decoration (IMD) injection molding process shown schematically

\* Mail address: Shih-Jung Liu, Department of Mechanical Engineering, Chang Gung University, 259, Wen-Hwa 1<sup>st</sup> Road, Tao-Yuan 333, Taiwan, ROC  
E-mail: shihjung@mail.cgu.edu.tw

2011b); and optimization (Yin et al., 2011; Deng et al., 2010, Gao and Wang, 2009; Zhang et al., 2009). The research efforts on IMD molded warpage, however, have been limited. Baek et al. (2008) studied the effect of processing conditions on the warpage of the film insert's molded parts. They found that the warpage decreased monotonically with increasing injection speed and exhibited a bell-shaped curve as a function of melt temperature. Chen et al. (2010) examined the effect of decoration film on mold surface temperature during the molding process and showed that the IMD process introduced asymmetric flow front advancement, uneven temperature distribution in the mold core and cavity, leading to severe residual stresses and warpage of parts. Recently, Larpsuriyakul and Fritz (2011) investigated warpage of injection molded in-mold labeling parts and found that it is the volume contraction difference between the label and substrate that forces IML parts to warp to the opposite side of the label. They also proposed that the IML part warpage problem can be dealt with by varying the temperatures of the stationary and moving mold platens.

This paper investigated, both experimentally and numerically, the warpage in IMD injection molded composites. All experiments were conducted on an 80-ton injection-molding machine. The materials used in the experiments included poly(ethylene terephthalate) (PET) films and 20% glass fiber filled PET resins. U-shaped parts with three different corner angles ( $90^\circ$ ,  $135^\circ$ , and  $150^\circ$ ) were molded, and the influence of various processing parameters on warpage was investigated. An experimental matrix was designed according to the experimental-parameter-design method developed by Taguchi (Peace, 1993). This approach statistically and ideally allows one to obtain the same results as a full-factorial experimental design would produce, but with fewer testing trials. In addition, a commercially available code (Moldex 3-D, 2011) was used to simulate the temperature distribution during the filling process and molded part warpage. A comparison was made between the molded and predicted warpage.

## 2 Experimental Procedure

The decoration films used for the experiments were commercially available poly(ethylene terephthalate) (PET) films (provided by Transart Graphics Inc., Taiwan), with a thickness of  $250\ \mu\text{m}$  and with pre-printed grids with a dimension of  $2\ \text{mm} \times 2\ \text{mm}$ . The resin used in this study was 20% glass fiber-filled polyethylene terephthalate (PET) (Nan-Ya Plastics, Taiwan). Before injection molding, the films were cut into specimens of  $100\ \text{mm}$  by  $40\ \text{mm}$  and formed to take the U-shapes of mold cavities, using a lab-scale thermoforming machine. They were then placed into the cavity for molding.

All experiments were conducted on an 80-ton injection-molding machine, with the highest injection rate of  $109\ \text{cm}^3/\text{s}$ . U-shaped plate cavities with a thickness of  $2\ \text{mm}$  and three different corner angles (i. e.,  $90^\circ$ ,  $135^\circ$ , and  $150^\circ$ ) were used for all experiments. Figure 2 shows the dimensions of the U-shaped plates, while Fig. 3 shows the layout of the mold cavity.

Four different processing parameters were selected as factors for evaluation, including melt temperature, mold temperature, melt injection pressure, and corner angles. To select the range of parameters for evaluation, a few test trials were first

completed to find the parameter ranges at which the parts could successfully be molded. Some arbitrary values were then chosen among these moldable parameter ranges for the subsequent statistical analysis. The melt temperature for the glass fiber-filled PET materials was maintained at  $270$ ,  $275$ , or  $280^\circ\text{C}$  (A melt temperature lower than  $270^\circ\text{C}$  led to short-shot molded parts, while a temperature higher than  $280^\circ\text{C}$  was found to thermally degrade the parts). The melt injection pressure was kept at  $83$ ,  $100$ , or  $125\ \text{MPa}$ . The mold temperature was set at  $55$ ,  $65$ , or  $75^\circ\text{C}$ . Finally, three corner angles, namely  $90^\circ$ ,  $135^\circ$ , and  $150^\circ$ , were selected to mold the parts. The injection rate was kept constant and set to  $97\ \text{cm}^3/\text{s}$ . Five specimens were evaluated in each test trial. The experiments consisted of 9 test trials, their design based on the L9 orthogonal array (Table 1) in the Taguchi approach (Peace, 1993). After molding, the warping angle ( $\phi$  in Fig. 2) of the molded parts was measured. The measured angles were then used for the subsequent statistical analysis.

## 3 Numerical Simulation

To better interpret the filling process and the temperature distribution of IMD injection molded parts, the IMD module of a commercially available code (Moldex 3-D, 2011) was used to simulate the temperature distribution during the filling process. During modeling, a U-shaped cavity was first modeled and a thin film was modeled in the cavity. The thermophysical properties of virgin PET (thermal conductivity  $k = 0.150\ \text{J/s m}^\circ\text{C}$ , density  $\rho = 1400\ \text{kg/m}^3$ , and heat capacity  $C_p = 1025\ \text{J/kg}^\circ\text{C}$ ) were adopted to model the decoration films. Figure 4A shows the solid modeling of the part, while Fig. 4B shows the layout of the mold and the cooling channels. The Cross-WLF model was employed to model the viscosity of the polymer melt. It

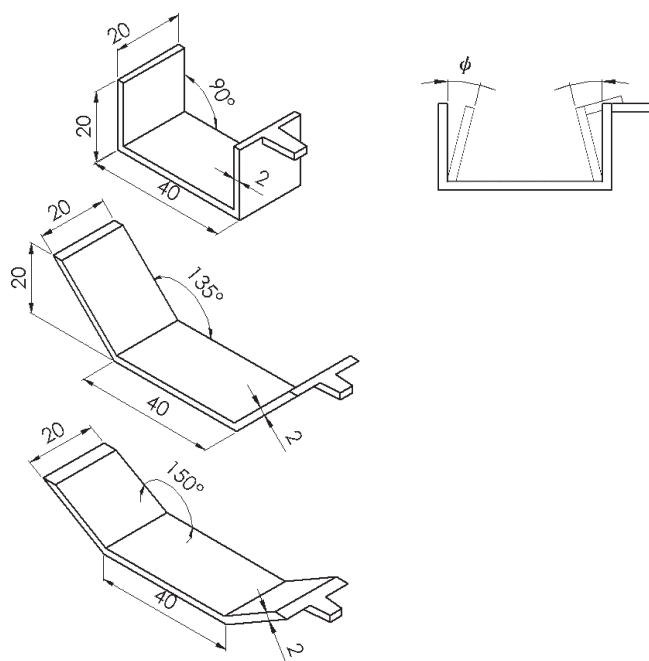


Fig. 2. Geometries and dimensions of the parts (unit: mm)

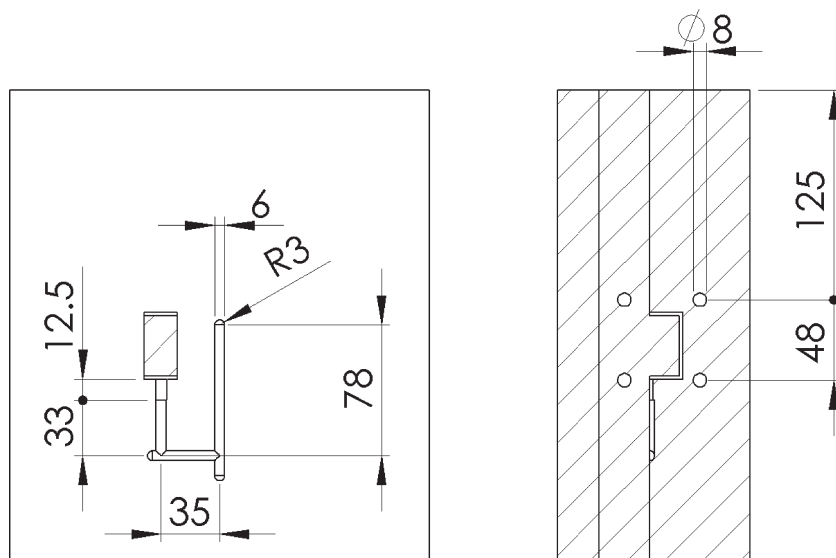


Fig. 3. Layout and dimensions of mold cavity (unit: mm)

Run	Melt temp. °C	Mold temp. °C	Injection pressure MPa	Corner angles degree	Specimen 1 degree	Specimen 2 degree	Specimen 3 degree	Specimen 4 degree	Specimen 5 degree	S/N dB
1	270	55	83	90	2.00	1.70	1.50	1.00	1.50	-3.94
2	270	65	100	135	2.75	2.45	2.50	2.45	2.50	-8.07
3	270	75	125	150	1.25	1.50	1.25	1.25	1.15	-2.18
4	275	55	100	150	1.75	1.25	1.35	1.35	1.50	-3.23
5	275	65	125	90	3.15	2.70	3.25	2.75	2.75	-9.33
6	275	75	83	135	2.35	2.75	1.85	1.50	1.50	-6.23
7	280	55	125	135	2.25	2.25	2.25	1.50	1.75	-6.13
8	280	65	83	150	1.00	1.25	1.25	1.10	1.00	-1.03
9	280	75	100	90	3.50	3.75	3.25	2.85	3.25	-10.46

Table 1. L'9 (3<sup>4</sup>) orthogonal array used in the experiments

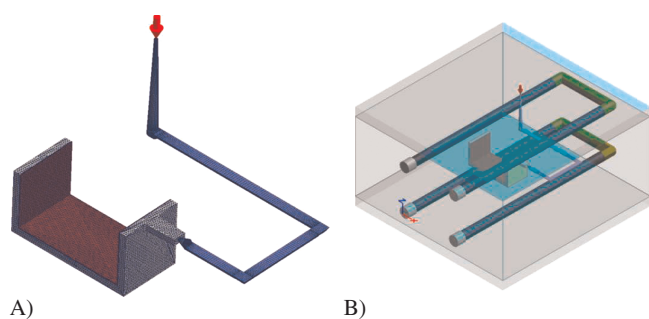


Fig. 4. (A) Solid modeling of the parts (B) computer model used to simulate the temperature distribution of the parts during cooling

describes the shear rate dependence of the upper Newtonian region, as well as the shear-thinning region of a shear viscosity curve. Figure 5 shows the temperature-dependent shear viscosity curves of the polymeric materials used. The thermophysical properties of the 20% glass fiber-filled PET used were: thermal conductivity  $k = 0.30 \text{ J/s m}^\circ\text{C}$ , density  $\rho = 1550 \text{ kg/m}^3$ , and heat capacity  $C_p = 2287 \text{ J/kg}^\circ\text{C}$ . With the initial melt tempera-

ture given and the boundary temperature assigned, the numerical iteration provides the temperature distribution inside the molded articles at different times. Further, to assess warpage of an injection-molded polymeric part, the program employs a simultaneous analysis of the compressible fluid flow, heat transfer, and residual stresses in the polymer during the filling and post-filling stages of the injection molding process and of mold cooling/heating that occurs throughout the entire process. Using the polymer temperature and pressure distributions as a function of time, an analysis was performed to predict the residual stresses and the part warpage (Moldex 3-D, 2011).

## 4 Results and Discussions

### 4.1 Effects of Processing Parameters on Molded Warpage

IMD experiments were completed using a commercial injection molding machine. Figure 6 shows photographically the IMD injection molded parts. All U-shaped plates warp toward the side of the decoration film. In addition, the 90° angled parts

exhibited the greatest amount of warpage, while the 150° angled parts showed the least amount of warpage. Furthermore, parts molded with decoration films exhibited more severe warpages than parts without the films did.

Furthermore, all molded warpages (warping angles) were measured and analyzed statistically. Table 1 lists the measurements of the properties for the 9 test trials in the experiments, designed based on the Taguchi method. The properties obtained from each test trial were analyzed statistically. In the analysis, a signal-to-noise (S/N) ratio indicates the statistical quantity, representing the power of a response signal, divided by the power of the variation in the signal due to noise. The S/N ratio was derived from the loss function and assumed different forms depending on the optimization objectives. The maximization of the S/N ratio led to minimization of any property that was sensitive to noise. Since the goal of optimization is minimization of warping angles, an equation incorporating the smaller-the-better characteristic can be used for the analysis:

$$\frac{S}{N} = -10 \log_{10} \left[ \left( \frac{1}{n} \right) \sum_{i=1}^n (y_i^2) \right], \quad (1)$$

where  $y_i$  is the measured warpage (i. e., the warping angle  $\varphi$  in Fig. 2), and  $n$  represents the number of samples in each test

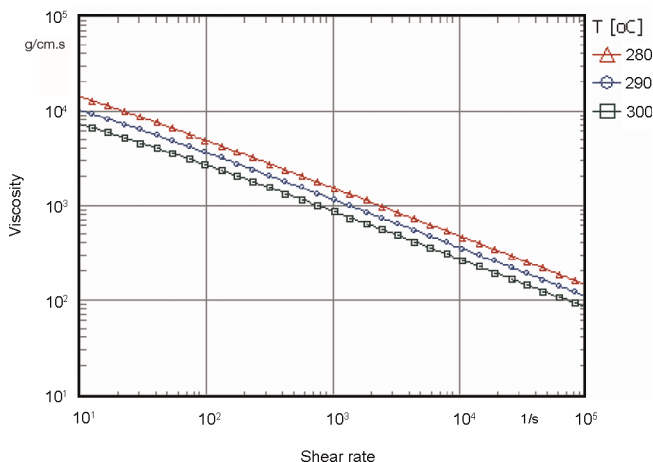


Fig. 5. Shear viscosity versus shear rate of 20% glass fiber-filled polyethylene terephthalate (PET) at different temperatures



Fig. 6. Photographs showing the IMD injection molded parts

trial (which is five in this study). The optimal factor levels, those with the largest S/N ratios, could then be obtained.

The variation in warpage for different processing parameters was analyzed according to the methods developed by Taguchi. The S/N ratios for the warpage of PET composites were calculated, and the results are shown in Fig. 7. Based on Fig. 7, the optimal factor levels that could statistically result in the minimum warpage within the selected processing ranges were predicted to be A1/B1/C1/D3. These optimized factor levels represented a melt temperature of 270 °C, a mold temperature of 55 °C, a melt injection pressure of 83 MPa, and a 150° corner angle.

The S/N ratio is a rather sensitive indicator, in that for every three decibel (dB) increase in S/N ratio, the error variation is halved relative to the signal. The significance of each factor in the main experiment can be judged by the change in S/N. Based on Fig. 7, the relative significance of each factor on warpage of IMD molded PET composites was arranged in decreasing order of corner angle ( $\Delta S/N = 5.765$  dB), injection pressure ( $\Delta S/N = 3.519$  dB), mold temperature ( $\Delta S/N = 1.858$  dB), and melt temperature ( $\Delta S/N = 1.535$  dB). For the factors selected in the main experiment, the corner angles of the parts and the melt injection pressure were found to be the most significant factors affecting the warpages of IMD composite parts.

#### 4.2 Numerical Simulation of Temperature and Part Warpage

To better understand the formation mechanism of part warpage, a commercially available code was employed to simulate the temperature distribution of molded parts at different times and predict the part warpages. Figure 8 shows the calculated temperature distributions in IMD molded parts without inserted films right after the completion of the melt filling, while Fig. 9 shows the temperature profiles in molded parts with the decoration films. Clearly the concave side of molded parts exhibited higher temperature distribution than the opposite side's temperature distribution. With the addition of the decoration film, the temperature gradient across the thickness increases

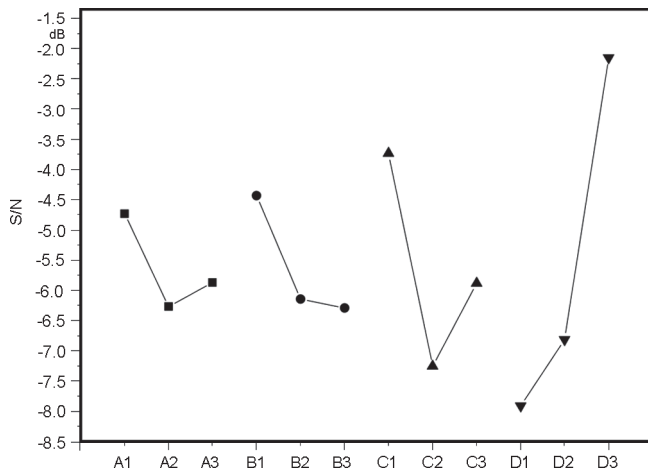
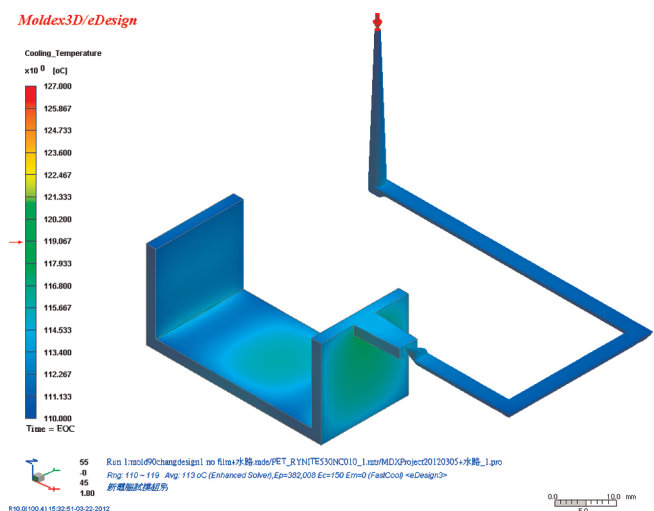
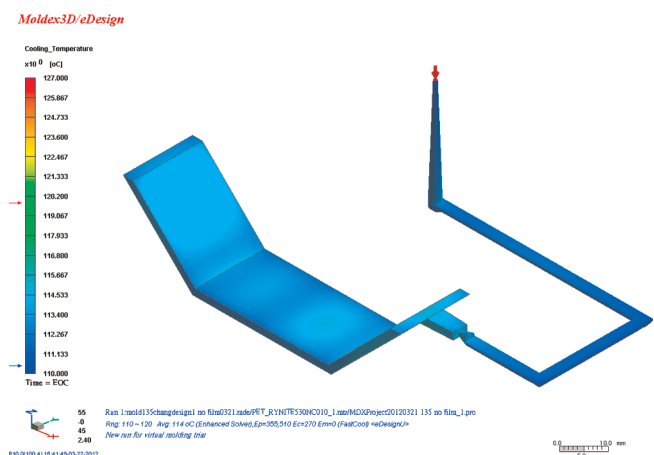


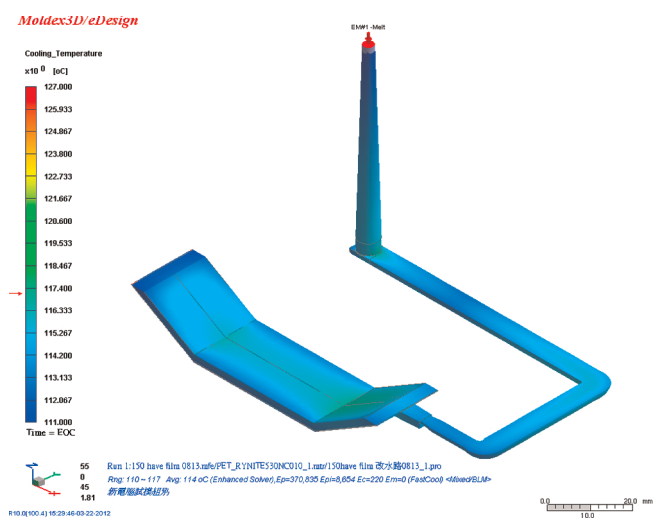
Fig. 7. Variation of the S/N ratio with factor level, (A) melt temperature, (B) mold temperature, (C) injection pressure (D) corner angle of the parts



A)

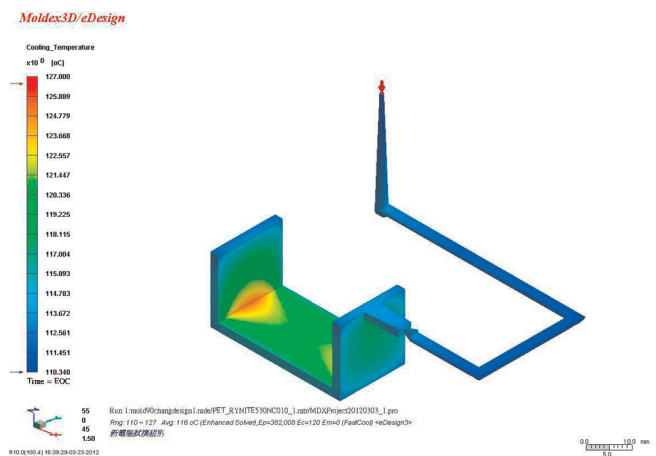


B)

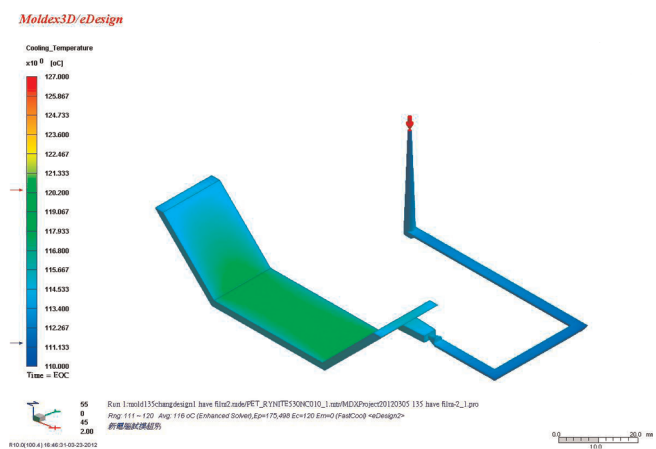


C)

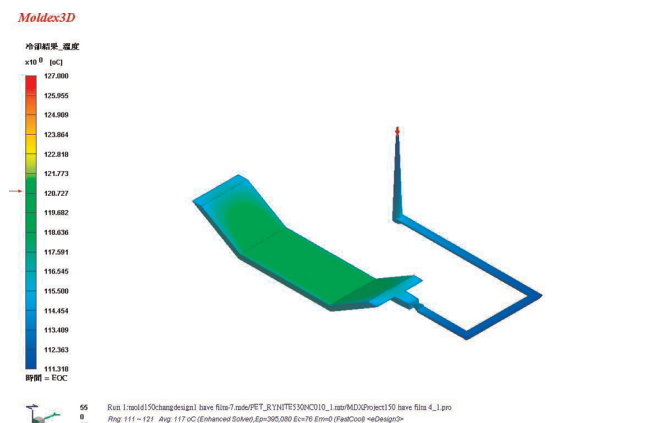
accordingly, with a higher temperature distribution at the film side. A higher temperature distribution leads to a slower cooling of the polymeric melts. The crystallinity and the relevant shrinkage at the film side (concave side) are higher than those at the opposite side. Molded parts may thus warp inward. The numerical results in Fig. 9 also show that the 90° angled parts



A)



B)



C)

Fig. 8. Temperature distribution of the injection molded parts with different corner angles (right after the completion of melt filling)

Fig. 9. Temperature distribution of the IMD injection molded parts of different corner angles (right after the completion of melt filling)

had the greatest temperature gradient across the thickness. This might explain why the molded 90° angled parts exhibited the greatest amount of warpage. Furthermore, a comparison has been made between the measured and the predicted warpages. Parts molded by the processing conditions of tests 1–3 in Table 1 were selected for comparison. The results in Table 2 show that the calculated warpage satisfactorily matched with the experimental data.

In the IMD injection molding process, the decoration film is first placed into the cavity, followed by the injection of hot polymer melt. The injected polymer melt starts to cool and solidify as soon as it touches the walls of the mold. The development of uneven residual stresses within the products leads to non-uniform differential shrinkages across the thickness, resulting in part warpage. In essence, both the thermal expansion coefficient and the stiffness of the materials, coupled with the transient temperature gradient within the material, drives the formation of residual stresses. Due to a differential thermal contraction (shrinkage) as the part cools, the thermal imbalance leads to a stress imbalance (typically compressive on the outsides of the plate and tensile on the inside of the plate). Relatively higher compressive stresses develop on the initially warmer side of the plate, thus causing the flat plate to bend (warp) towards the direction of where the higher temperature is.

From Fig. 8, it is noted that the temperatures are higher at the inner side (concave side) of the part, compared to the temperatures at the outer sides. Since the temperature distribution at the inner side is higher, the polymer materials tend to cool down slower and result in higher crystallinity. The shrinkage of the materials at the inner side is greater, and thus results in parts warping toward the inner side. Furthermore, due to the poor thermal conductivity of the PET films, the temperature gradient across the thickness of the parts increased with the insertion of the films, as shown in Fig. 9. This in turn led to more severity of warpages of molded parts.

The experimental data suggested that the corner angles of the parts have the most significant effect on part warpage. The 90° angled parts exhibited the greatest amount of warpage, while the 150° angled parts showed the least amount of warpage. This can be explained by the fact that the parts with 90° corner angles have the greatest thermal gradients across the thickness, as shown in Fig. 8 and 9. These molded parts thus exhibited the greatest warpage. The 150° corner angle parts, on the contrary, have the least uneven temperature distributions across the thickness, and thus showed the smallest warpages.

Decreasing the melt filling pressure helped reduce the warpage in IMD molded parts. This might be due to the fact that a

higher filling pressure helps push the molten polymer against the mold wall for cooling. The cooling rate increases accordingly. As the cooling rate of the injection molding process increases, the unbalanced residual stress caused by the thermal gradient across the part thickness increases as well. The induced part warpage increases accordingly.

The melt temperature was found to increase the warpages of IMD molded parts, as suggested by the experimental results in Fig. 7. Increasing the melt temperature decreases the cooling rate of the parts. The polymeric materials take more time to cool. The level of crystallinity of the materials increases accordingly. This in turn leads to greater shrinkage of the polymeric materials and warpages of the molded part. However, the warpage increases again as the melt temperature is above 275 °C. This matches with the results of Baek et al. (2008) with a “bell-shaped” tendency of part warpage. This can be explained by the fact that a higher melt temperature keeps the polymeric melt hot for a longer time. This in turn keeps the filling gate from frozen and helps pack the materials to reduce the shrinkage and warpage of molded parts.

Increasing the mold temperature keeps the polymer melt at high temperatures for a longer amount of time. The level of crystallinity of the materials increases. Parts of larger shrinkage and warpage can then be molded. Therefore, a low mold temperature should be adopted to minimize the molded part warpages, as suggested by the experimental results in Fig. 7.

Product warpage caused by inappropriate mold design and/or processing conditions is a recurrent problem during the injection molding of IMD parts. The warpage can be largely the results of thermally induced effects which arise during the mold cooling (solidification) stages of the manufacturing process. The magnitude of these effects is coupled to the geometry of the mold cavity, the thermophysical properties of the decoration films and the viscous flow behavior of the polymers. Experimental design based on the Taguchi method was appropriate in minimizing warpage of IMD molded parts by optimizing the processing variables, although the approach may not be able to catch the high order interactions between and among factors. Experimental investigation and numerical simulation of an IMD warpage problem can be used to guide corrective measures if the problem arises, and to prevent a potential problem from occurring in the first place.

## 5 Conclusions

This report has examined the influence of processing parameters on the warpage of IMD injection molded composite parts.

Run	Melt temperature °C	Mold temperature °C	Injection pressure MPa	Corner angles degree	Measured warpage degree	Calculated warpage degree
1	270	55	83	90	1.54	1.43
2	270	65	100	135	2.53	2.49
3	270	75	125	150	1.28	1.18

Table 2. A comparison of the measured and calculated warpages for the IMD molded parts

The experimental results suggested that all molded parts warped toward the side of the decoration film. For the parameters selected in the experiments, the corner angle of molded parts and the melt injection pressure were found to be the principal factors in affecting the warpage of IMD injection molded parts. The 90° angled parts exhibited the greatest amount of warpage, while the 150° angled parts showed the least amount of warpage. In addition, a numerical simulation, using commercially available software, has been carried out to simulate the melt temperature distributions during the filling process and to better interpret the formation mechanism of warpages in IMD injection molded parts; with this, steps can thus be taken to optimize the part design and processing parameters. This optimization would provide significant advantages in improving the quality of parts.

## References

- Baek, S. J., Kim, S. Y., Lee, S. H., Youn, J. R., Lee, S. H., "Effect of Processing Conditions on Warpage of Film Insert Molded Parts", *Fiber Polym.*, **6**, 747–754 (2008), DOI:10.1007/s12221-008-0117-y
- Chen, S. C., Li, H. M., Huang, S. T., Wang, Y. C., "Effect of Decoration Film on Mold Surface Temperature During In-Mold Decoration Injection Molding Process", *Inter. Comm. Heat Mass Trans.*, **37**, 501–505 (2010), DOI:10.1016/j.icheatmasstransfer.2010.01.005
- Chiang, Y.-C., Cheng, H.-C., Huang, C.-F., Lee, J.-L., Lin, Y., Shen, Y.-K., "Warpage Phenomenon of Thin-wall Injection Molding", *Int. J. Adv. Manuf. Tech.*, **55**, 517–526 (2011), DOI:10.1007/s00170-010-3106-4
- Defosse, M., "In-Mold Decoration – Harbors Huge Potentials", *Modern Plast.*, **78**, 76–77 (2001)
- Deng, Y.-M., Zhang, Y., Lam, Y. C., "A Hybrid of Mode-Pursuing Sampling Method and Genetic Algorithm for Minimization of Injection Molding Warpage", *Mater. Design*, **31**, 2118–2123 (2010), DOI:10.1016/j.matdes.2009.10.026
- Peace, G. S.: *Taguchi Methods*, Addison-Wesley, New York (1993)
- Gao, Y., Wang, X., "Surrogate-based Process Optimization for Reducing Warpage in Injection Molding", *J. Mater. Process. Tech.*, **209**, 1302–1309 (2009), DOI:10.1016/j.jmatprotec.2008.03.048
- Kovacs, J. G., Solymossy, B., "Effect of Glass Bead Content and Diameter on Shrinkage and Warpage of Injection Molded PA6", *Polym. Eng. Sci.*, **49**, 2218–2224 (2009), DOI:10.1002/pen.21470
- Larpsuriyakul, P., Fritz, H.-G., "Warpage and Countermeasure for Injection Molded In-Mold Labeling Parts", *Polym. Eng. Sci.*, **51**, 411–418 (2011), DOI:10.1002/pen.21849
- Lee, S. H., Kim, S. Y., Youn, J. R., Kim, B. J., "Warpage of A Large-sized Orthogonal Stiffened Plate Produced by Injection Molding and Injection Compression Molding", *J. Appl. Polym. Sci.*, **116**, 3460–3467 (2010)
- Leong, Y. W., Kotaki, M., Hamada, H., "Effects of the Molecular Orientation and Crystallization on Film-substrate Interfacial Adhesion in Poly(ethylene terephthalate) Film-insert Moldings", *J. Appl. Polym. Sci.*, **104**, 2100–2107 (2007), DOI:10.1002/app.25620
- Liu, F., Zhou, H., Li, D., "Numerical Simulations of Residual Stresses and Warpage in Injection Molding", *J. Reinf. Plast. Comp.*, **28**, 571–585 (2009)
- Liu, S. J., Hsu, C. M., Chang, P. W., "Parameters Affecting the Ink Wash-off in In-Mold Decoration of Injection Molded Parts", *Int. Polym. Proc.*, **27**, 224–230 (2012), DOI:10.3139/217.2506
- Ozcelik, B., Sonat, I., "Warpage and Structural Analysis of Thin Shell Plastic in the Plastic Injection Molding", *Mater. Design*, **30**, 367–375 (2009), DOI:10.1016/j.matdes.2008.04.053
- Puentes, C. A., Okoli, O. I., Park, Y. B., "Determination of Effects of Production Parameters on the Viability of Polycarbonate Films for Achieving In-Mold Decoration in Resin Infused Composite Components", *Comp. A-Appl. Sci. Manuf.*, **40**, 368–375 (2009), DOI:10.1016/j.compositesa.2008.12.018
- User's Manual, *Moldex 3-D*, Taipei, Taiwan (2011)
- Wong, A. C. Y., Liang, K. Z., "Thermal Effects on the Behaviours of PET Films Used In The In-Mould-Decoration Process Involved In Plastics Injection Molding", *J. Mater. Process. Technol.*, **63**, 510–513 (1997), DOI:10.1016/S0924-0136(96)02674-X
- Yin, F., Mao, H., Hua, L., Guo, W., Shu, M., "Back Propagation Neural Network Modeling for Warpage Prediction and Optimization of Plastic Products during Injection Molding", *Mater. Design*, **32**, 1844–1850 (2011), DOI:10.1016/j.matdes.2010.12.022
- Zhang, Y., Deng, Y.-M., Sun, B.-S., "Injection Molding Warpage Optimization Based on A Mode-pursuing Sampling Method", *Polym. Plast. Tech. Eng.*, **48**, 767–774 (2009), DOI:10.1080/03602550902824663
- Zhou, H., Wang, Z., Li, J., Li, D., "A Surface Model-based Simulation for Warpage of Injection-molded Parts", *Polym. Eng. Sci.*, **51**, 785–794 (2011), DOI:10.1002/pen.21884
- Zhou, H., Zeng, S., Wang, Z., Li, J., Cui, S., "Warpage Simulation of Plastic Injection Moulded Parts Using A Multi-point Constraint Approach", *Mater. Res. Innov.*, **15**, 237–240 (2011), DOI:10.1179/143307511X12858957673590

## Acknowledgements

The National Science Council of Taiwan, R.O.C., under the grant NSC98-2221-E-182-003-MY3, has supported this work financially.

*Date received: July 22, 2012*

*Date accepted: December 10, 2012*

Bibliography  
DOI 10.3139/217.2690  
Intern. Polymer Processing  
XXVIII (2013) 2; page 221–227  
© Carl Hanser Verlag GmbH & Co. KG  
ISSN 0930-777X

You will find the article and additional material by entering the document number **IPP2690** on our website at [www.polymer-process.com](http://www.polymer-process.com)